EPIDEMIOLOGY

Identifying the Interaction Between Influenza and Pneumococcal Pneumonia Using Incidence Data

Sourya Shrestha,[1,2]* Betsy Foxman,[3] Daniel M. Weinberger,[4,5] Claudia Steiner,[6] Cécile Viboud,[4] Pejman Rohani[1,2,7]

The association between influenza virus and the bacterium *Streptococcus pneumoniae* (pneumococcus) has been proposed as a polymicrobial system, whereby transmission and pathogenicity of one pathogen (the bacterium) are affected by interactions with the other (the virus). However, studies focusing on different scales of resolution have painted an inconsistent picture: Individual-scale animal experiments have unequivocally demonstrated an association, whereas epidemiological support in human populations is, at best, inconclusive. We integrate weekly incidence reports and a mechanistic transmission model within a likelihood-based inference framework to characterize the nature, timing, and magnitude of this interaction. We find support for a strong but short-lived interaction, with influenza infection increasing susceptibility to pneumococcal pneumonia ~100-fold. We infer modest population-level impacts arising from strong processes at the level of an individual, thereby resolving the dichotomy in seemingly inconsistent observations across scales. An accurate characterization of the influenza-pneumococcal interaction can form a basis for more effective clinical care and public health measures for pneumococcal pneumonia.

INTRODUCTION

It is increasingly clear that many pathogens interact. Infection with one pathogen can affect the severity, infectivity, or susceptibility to subsequent infection with other pathogens, and these effects can have profound clinical, epidemiological, and evolutionary implications (*1*–*8*). An important example is the putative association between the influenza virus and the bacterium *Streptococcus pneumoniae* (pneumococcus). Suspicions concerning a possible interaction among the two date back over two centuries, with the observation that prevalence of pneumonia increased during influenza epidemics (*9*). Histopathological examinations have demonstrated that at least 24% of fatalities during the 1918 Spanish influenza pandemic had evidence of concomitant pneumococcal respiratory infection (*10*). More recently, an atypical increase in pneumococcal hospitalizations coincided with the occurrence of the A/H1N1 influenza pandemic in fall 2009 (*11*). During nonpandemic periods, the epidemiology of these pathogens is characterized by peaks during the winter months in temperate countries (*12*–*14*), as can be seen from long-term weekly epidemiological records for the state of Illinois, United States, before and after the introduction of pneumococcal conjugate vaccines (PCVs) in 2000 (*15*) (see Fig. 1).

There is a discrepancy in our understanding of this interaction, arising from the different scales at which it has been studied. The evidence garnered at the level of the individual is both consistent and strong. In humans, histopathological examinations have implicated secondary bacterial infections in lethal (*10*, *16*–*19*) and severe influenza cases (*11*). In animal models, challenge experiments have shown that previous influenza infection enhances the severity (*20*–*22*) and susceptibility (*23*, *24*) of subsequent pneumococcal infection. At the population level, however, comparative analyses of seasonal patterns of influenza and pneumococcal pneumonia incidence either have revealed a modest association (*25*, *26*) or fail to expose any signature of interaction (*27*) (see section S-2 in the Supplementary Materials for more discussion). One possible explanation for these contrasting findings is that conclusions drawn from animal challenge experiments are not directly relevant to human pathogen systems. Alternatively, the mechanisms identified in animal models may be in operation, but their dynamical footprints in epidemiological data may be too subtle to detect using traditional methodologies. To resolve this dichotomy, here, we confronted a mechanistic transmission model with incidence reports of influenza and pneumococcal pneumonia within a likelihood-based statistical inference framework. This approach permitted not only the quantification of central parameters but also the rigorous testing of alternative hypotheses.

Our aim was to identify the nature, strength, and timing of the putative interaction between influenza and pneumococcal pneumonia. We examined three distinct hypotheses. The first (**H1**: transmission impact) proposes that individuals infected with pneumococcal pneumonia contribute more to pneumococcal transmission if they have been recently infected with influenza. The second (**H2**: susceptibility impact) proposes that individuals infected with influenza are more susceptible to pneumococcal pneumonia. The third (**H3**: pathogenesis impact) proposes that influenza infection only affects the pathogenesis of subsequent pneumococcal pneumonia infection, enhancing the severity of clinical symptoms and thereby increasing the odds of notification.

[1]Department of Ecology and Evolutionary Biology, University of Michigan, Ann Arbor, MI 48109, USA. [2]Center for the Study of Complex Systems, University of Michigan, Ann Arbor, MI 48109, USA. [3]Department of Epidemiology, University of Michigan, Ann Arbor, MI 48109, USA. [4]Division of International Epidemiology and Population Studies, National Institutes of Health, Bethesda, MD 20892, USA. [5]Department of Epidemiology of Microbial Diseases, Yale School of Public Health, New Haven, CT 06520, USA. [6]Healthcare Cost and Utilization Project, Center for Delivery, Organization and Markets, Agency for Healthcare Research and Quality, U.S. Department of Health and Human Services, Rockville, MD 20850, USA. [7]Fogarty International Center, National Institutes of Health, Bethesda, MD 20892, USA.
*Corresponding author. E-mail: sourya@umich.edu

RESULTS

Model

We formulated these focal hypotheses within an *SIRS* compartmental model (*28*, *29*) of pneumococcal transmission using influenza incidence as a covariate. Our pneumococcal transmission model split the host population into three compartments according to their pneumococcal

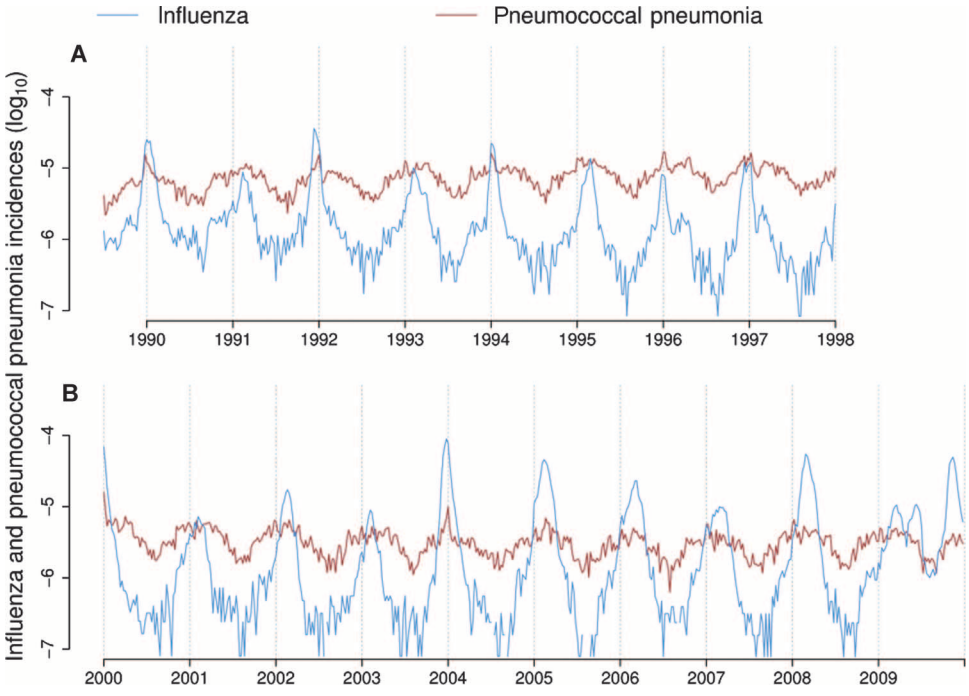

Fig. 1. Weekly incidences of influenza and pneumococcal pneumonia in Illinois. (A and **B)** Before (A, data set I) and after (B, data set II) the introduction of PCVs. Incidences are the weekly hospitalization case reports as a fraction of the total population (see Materials and Methods for details).

infection status: with *S*, *I*, and *R* representing susceptible, infectious, and recently recovered individuals. Compartments *S* and *I* are further subdivided to take into account individual status with respect to influenza. Specifically, S_F and I_F represent susceptible and infectious individuals currently infected with influenza, whereas S_U and I_U have no recent history of influenza. The model is schematically represented in Fig. 2A. We estimated the size of S_F, assuming it is proportional to the current influenza incidence, corrected for underreporting. That is, at time *t*, $S_F(t) = \frac{F(t)}{\rho_F N(t)} S(t)$, where $N(t)$ is the population size, $F(t)$ is the number of reported influenza cases, and ρ_F is the reporting probability.

In our model, susceptibles experienced a per capita hazard of pneumococcal infection, $\lambda(t)$, that comprised two sources of transmission: (i) those currently experiencing acute pneumococcal pneumonia and (ii) a contribution from long-term bacterial carriage, modeled as a constant, ω, yielding $\lambda(t) = \beta(t)\left[\frac{I(t)}{N(t)} + \omega\right]$. Here, $\beta(t)$ represents seasonally varying transmission rate. Our pneumococcal transmission model was implemented as a Markov chain, incorporating both demographic and extrademographic noise (*30*), together with a probabilistic reporting process, with reporting probability ρ_P. The complete model is described in Materials and Methods.

Hypotheses formulation

To formulate **H1**—increased transmission of pneumococcus as a result of influenza infection—we distinguished between the transmission contribution of those infected with pneumococcal pneumonia according to their status with respect to influenza. Specifically, we assumed that the pneumococcal transmission rate of individuals recently infected with influenza is modulated by a factor θ, relative to those uninfected with influenza, such that $\lambda(t) = \beta(t)\left[\frac{I_U}{N} + \theta\frac{I_F}{N} + \omega\right]$. Thus, **H1** implies $\theta > 1$, with the null hypothesis given by $\theta = 1$. To formulate **H2**—influenza infection increases susceptibility to pneumococcal pneumonia—we assumed that the relative hazard rates of susceptibles in the subcompartments, S_U and S_F, are given by $\lambda(t)$ and $\phi\,\lambda(t)$, respectively. The hazard ratio ϕ is then a measure of the susceptibility impact of influenza infection. Again, **H2** implies $\phi > 1$, with the null hypothesis $\phi = 1$. Finally, to formulate **H3**—increased pneumococcal pneumonia severity because of influenza infection—we hypothesized that individuals co-infected with influenza only develop more severe symptoms and are, therefore, ξ times more likely to be reported. Hypothesis **H3** implies $\xi > 1$, with $\xi = 1$ being the null. To evaluate the empirical evidence in support of each model, we carried out formal hypothesis testing using likelihood-based inference (*31*–*33*) (see Materials and Methods for details), applied to weekly epidemiological records of influenza and pneumococcal pneumonia hospitalizations from Illinois. Further, we tested the impact of the introduction of the pneumococcus vaccination program on these interactions by fitting separate models to data from the prevaccination (data set I, Fig. 1A) and vaccination time periods (data set II, Fig. 1B). For each hypothesis, we constructed likelihood profiles for the focal parameters (θ, ϕ, and ξ); that is, we systematically varied the parameter while maximizing the likelihood over all other parameters. This approach not only yields the maximum likelihood estimates (MLEs) but also provides the corresponding 95% confidence intervals (CIs) for the parameter profiled.

Nature, timing, and the intensity of the interaction

The results concerning the nature of the interaction between influenza and pneumococcal pneumonia were unequivocal in our study. We found no evidence to support the transmission (**H1**) or severity (**H3**) hypotheses in either data set (Fig. 2, B and D, and E and G, respectively). The 95% CIs for θ (data set I: 0.41 to 4.7; data set II: 0.3 to 1.9) and for ξ (data set I: 0.4 to 3.4; data set II: 0.38 to 1.4) include the null expectation of 1. In contrast, we find the susceptibility impact ϕ to be considerably larger than one in both data sets (data set I: 53 to 230; data set II: 83 to 280). In the absence of support for **H1** and **H3**, and for reasons of parsimony, we reestimated the susceptibility impact ϕ for each data set after setting θ and ξ to 1 (insets of Fig. 2, C and F). The MLE of ϕ—quantifying the magnitude of the susceptibility impact of influenza on pneumococcal pneumonia—is 115 (CI, 70 to 230) in data set I and 85 (CI, 27 to 160) in data set II (MLEs are presented in table S2 of the Supplementary Materials). We also established the time scale of the interaction by producing a likelihood profile for the susceptibility factor when the window of interaction is extended, with influenza preceding pneumococcus superinfection by up to 3 weeks (see S-1.2 in the Supplementary Materials for details). As shown in fig. S6, there is no evidence in support of the interaction extending beyond 1 week. Simply put, our analyses identified a transient but significant (~100-fold) increase in the risk of pneumococcal pneumonia after influenza infection.

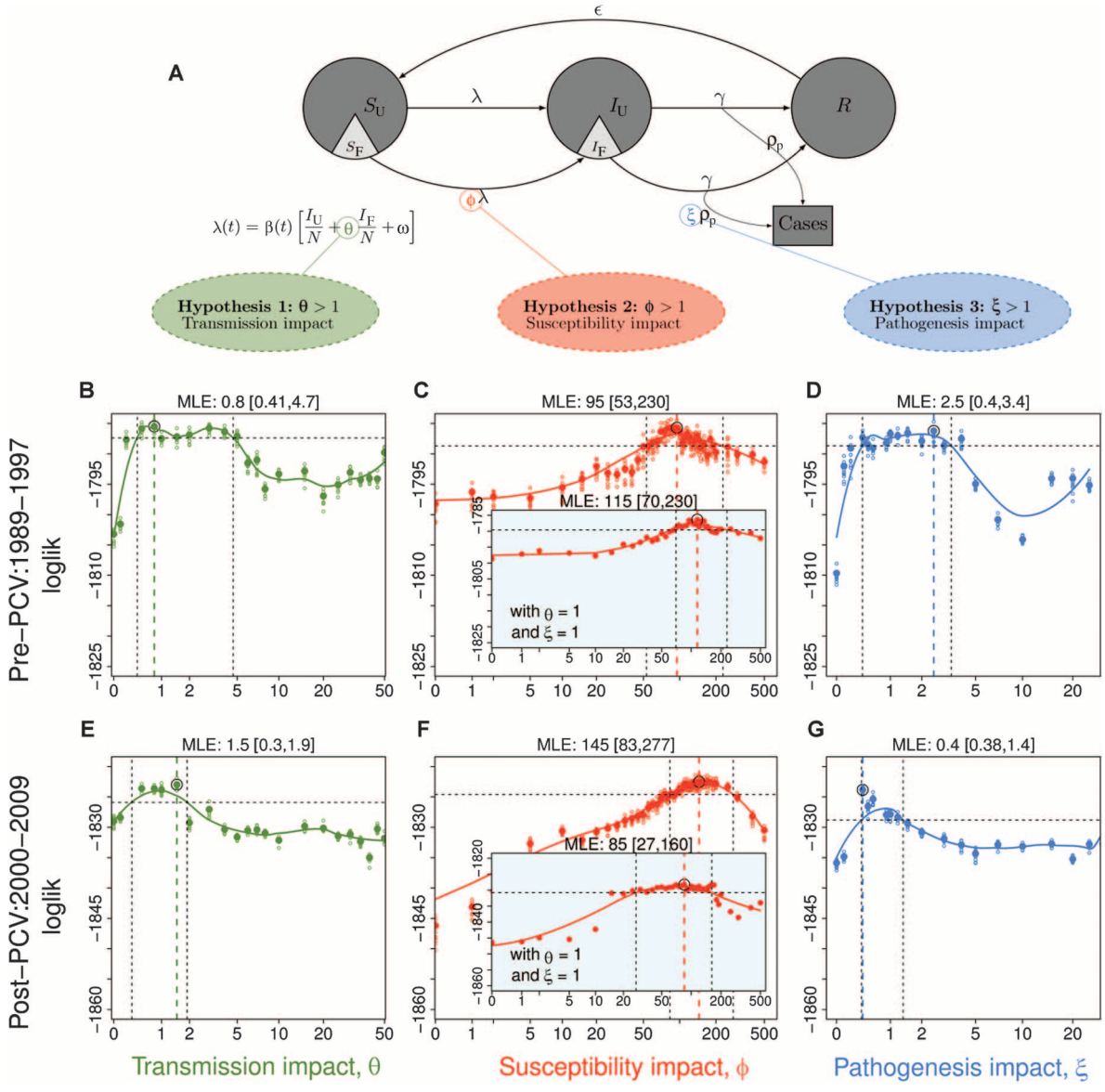

Fig. 2. The nature and intensity of influenza-pneumococcal interaction. (**A**) Schematic representation of the pneumococcal transmission model. Following the *SIRS* framework, individuals progress along $S \rightarrow I \rightarrow R \rightarrow S$ at per capita rates λ, γ, and ε, respectively. Progression of individuals recently infected with influenza is tracked separately via classes S_F and I_F. Pneumococcal pneumonia case reports are fraction of the infected as they recover. Births and deaths are present in the model but omitted in this illustration for clarity (see Materials and Methods for the complete model). We test three hypothesized pathways of influenza-pneumococcal interaction. **H1** (θ > 1): Individuals infected with pneumococcal pneumonia contribute more to pneumococcal transmission if they have been recently infected with influenza. **H2** (ϕ > 1): Individuals recently infected with influenza are more susceptible to pneumococcal pneumonia. **H3** (ξ > 1): Individuals infected with pneumococcal pneumonia are more likely to be reported, if recently infected with influenza. (**B** to **G**) Nature and intensity of interactions between influenza and pneumococcal pneumonia, inferred in Illinois from 1990 to 1997 (B to D, data set I) and 2000 to 2009 (E to G, data set II). Arranged column-wise are the tests for the three hypotheses **H1**, **H2**, and **H3**. Plotted in each graph are likelihood profiles for the respective parameters—the profiles are created by fitting a smooth line through the log of the arithmetic mean likelihoods (shown in colored filled circles) in 10 repeated likelihood estimates (shown in colored empty circles). The values within the two dashed black lines are within the estimated 95% CI, and the value marked with dashed colored line represents the MLE. The values corresponding to the MLE and the 95% CIs are given on the top margin of the graphs. The 95% CI is taken to be $\chi^2_1(0.95)/2 \approx 1.92$ log-likelihood units below the maximum—univariate confidence limits using the χ^2 distribution. For each of the three parameters, value of 1 represents the null hypothesis. For **H2**, we show the profiles with θ = 1, and ξ = 1 (that is, after rejecting **H1** and **H3**) in the inset graphs.

Epidemiological impact

We translate our MLEs within an epidemiological context by calculating the etiologic fraction of pneumococcal cases, defined as the proportion of cases that is attributable to the interaction with influenza (see Materials and Methods for details). We found substantial variation in this quantity (Fig. 3), with the etiologic fraction accounting for

up to 40% of pneumococcal cases during peak influenza season, but is generally low (typically <1%) otherwise. On an annual basis, the etiologic fraction is 2 to 10%, consistent with values estimated elsewhere from epidemiological time series methods (*11*, *25*). This translated to an estimated 2172 [1567, 2891] and 1077 [782, 1430] cases of pneumococcal hospitalizations that could be attributed to influenza in data sets I and II, respectively.

As a validation step, we compared simulations arising from the MLE and the null models with the data (figs. S3 to S5). We found that although ignoring the impact of influenza infection on pneumococcal epidemiology generates dynamics that reproduce the seasonal patterns in pneumococcal pneumonia cases, these fail to capture the observed interannual variability in peak sizes. Accounting for the interaction with influenza explained some of this variability, as reflected in improved goodness-of-fit statistics (R^2 increased from 0.687 to 0.739 in data set I, and from 0.523 to 0.618 in data set II; fig. S5). The modest increase in R^2 after the inclusion of influenza-pneumococcal interaction highlights the subtlety of its dynamical signature and perhaps helps to explain its elusiveness in previous epidemiological analyses.

Consequences of detection

Finally, we explored the consequences of the influenza-pneumococcal interaction we have detected for pneumococcal epidemiology. We wished to examine the dynamical impact of variability in seasonal influenza peaks on excess pneumococcal cases. To do this, we first manufactured multiple hypothetical influenza data sets that differed in the interannual variability in their peak sizes by a factor of up to 50 (for example, Fig. 4, B to F). Then, using these synthetic influenza data as a covariate, we simulated our pneumococcal transmission model using MLE parameters (see Materials and Methods for details on inference using manufactured data). We found the magnitude of pneumococcal pneumonia peaks to be relatively insensitive to moderate year-to-year variation in the size of influenza outbreaks (Fig. 4A). For instance, a doubling of influenza peak resulted in less than 25% increase in the magnitude of pneumococcal peak. The influenza peak would need to be ~20-fold larger than baseline to generate a doubling of the pneumococcal peak (Fig. 4A).

This observation has implications for the ability to detect influenza-pneumonia interaction in epidemiological data; the identifiability of ϕ depends on variability in the peak influenza incidence. To illustrate, we manufactured five sets of weekly influenza case reports spanning a 4-year period, with different magnitudes of epidemic in year 3, marked as I to V in Fig. 4A. For each influenza data set (Fig. 4, B to F), we constructed pneumococcal pneumonia incidences (Fig. 4, G to K) by simulating the MLE model with the manufactured influenza data set as a covariate. Then, using these simulated influenza and pneumococcal pneumonia incidence data, we attempted to infer the interaction parameter ϕ using our likelihood-based inference framework (see Materials and Methods for details). Even in this optimistic scenario, with perfect knowledge of pneumococcal epidemiology and host demography, we find that it is not possible to detect any interaction unless the influenza outbreak in year 3 is at least fourfold larger than the seasonal baseline (Fig. 4, L to P). This result is robust to some variability in the timing of the influenza peaks (see fig. S10). It is also worth noting that the variability observed in the Illinois

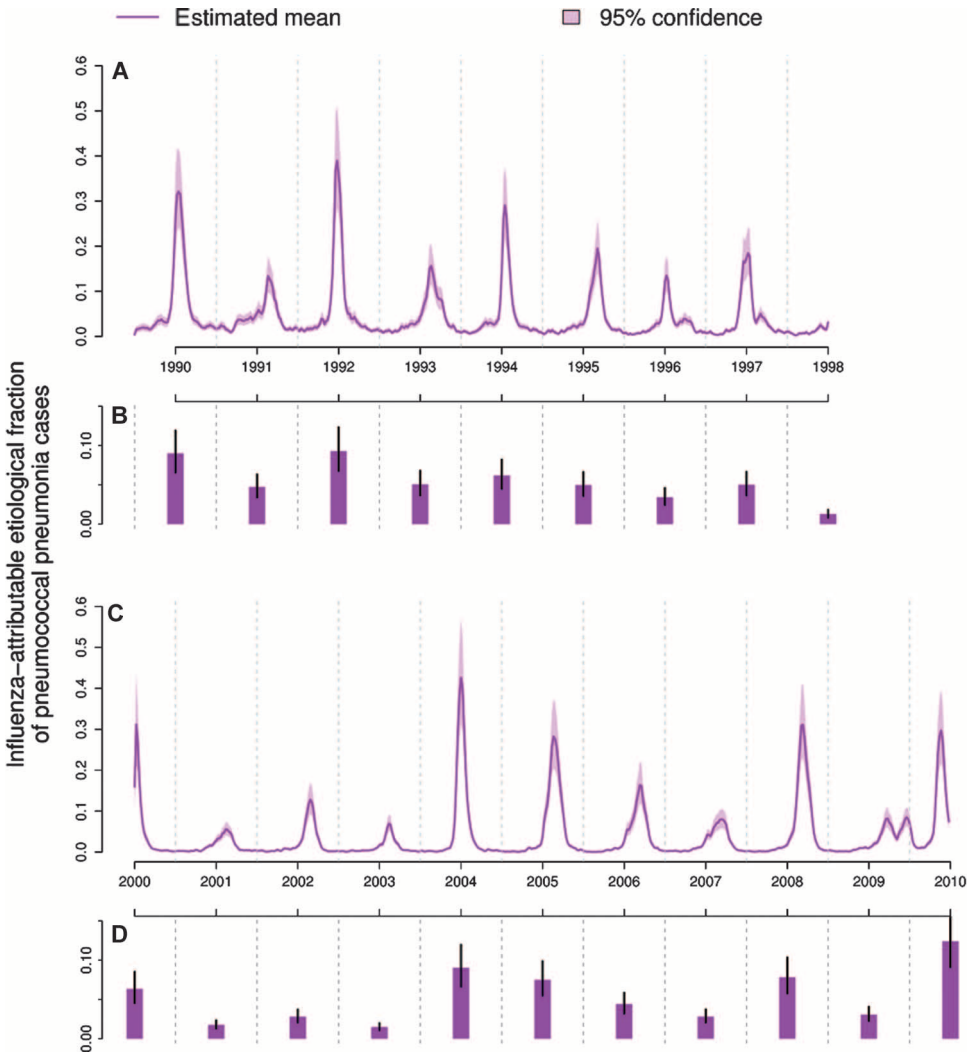

Fig. 3. Impact of influenza on pneumococcal epidemiology. (**A** to **D**) Estimates of influenza-attributable etiological fraction of pneumococcal pneumonia cases in Illinois in data set I (A and B) and data set II (C and D). The estimates are based on the corresponding MLE models for each data set. (B and D) Fractions averaged over annual periods, midyear to midyear, for intervals shown in (A) and (C), respectively. Influenza-attributable etiological fraction of pneumococcal pneumonia cases in any time interval is taken to be the ratio of pneumococcal cases as a result of influenza to the total pneumococcal cases in the given time interval. The estimates for data sets I and II are based on 1000 replicate simulations of the respective MLE models (see Materials and Methods for details on the calculation of etiological fractions).

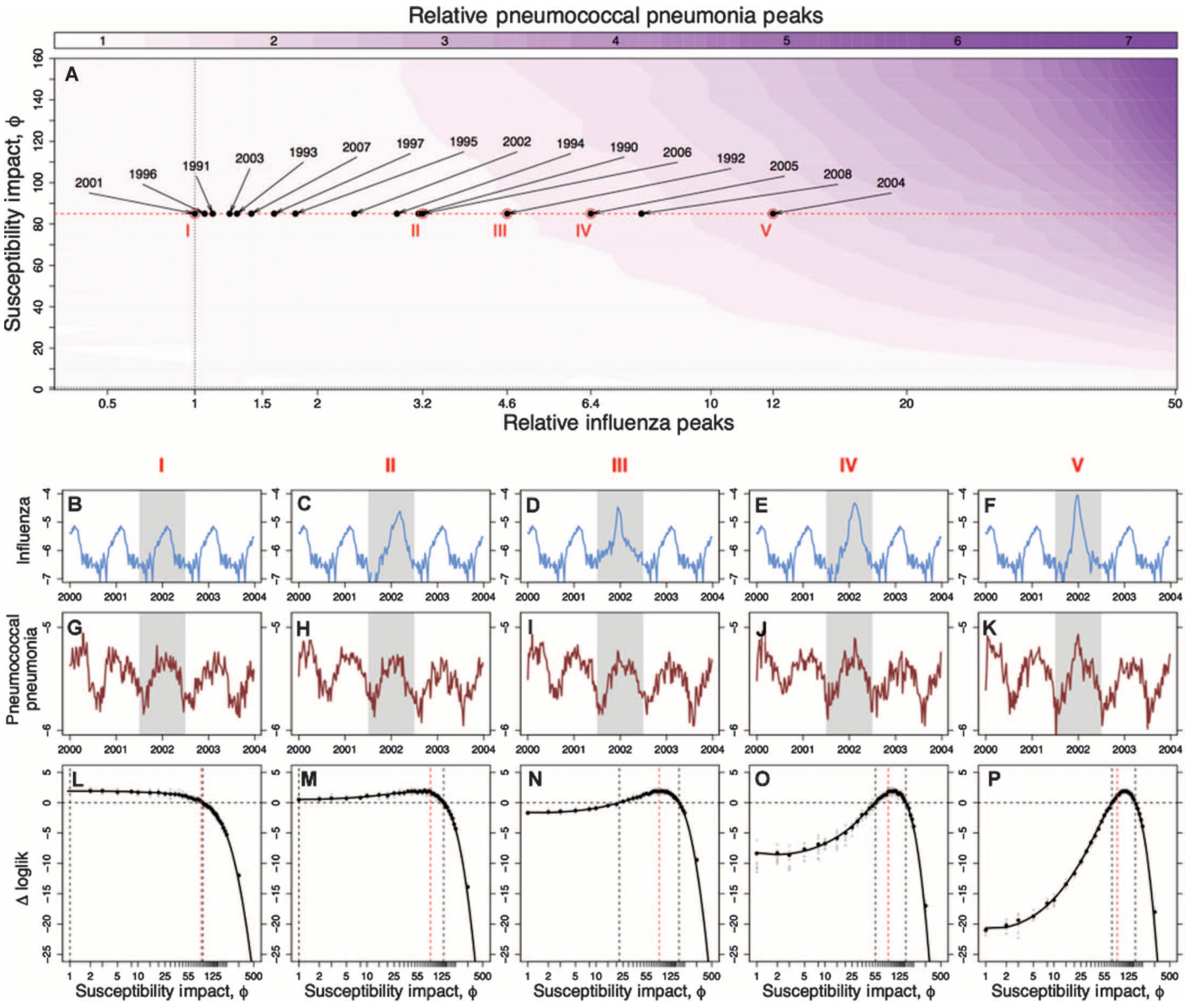

Fig. 4. Detectability of influenza-pneumococcal interaction in manufactured data. We manufactured multiple hypothetical influenza data sets that differ in their interannual variability in peak sizes. On the basis of the MLE model, we then predicted pneumococcal pneumonia incidences for each influenza data set. (**A**) Color-coded contours represent the magnitude of annual peaks in pneumococcal pneumonia incidences when the annual peaks in influenza incidences (plotted on the horizontal axis) and susceptibility impact ϕ (plotted on the vertical axis) vary. Magnitude of both influenza and pneumococcal pneumonia peaks is presented as fold increase relative to their respective baseline peaks. Marked in filled circles are where actual annuals peaks in the data lie. We then sampled five scenarios (I to V), indicated by five open red circles. Plotted column-wise are inference tests performed on these five sets of manufactured data in each of the scenarios (see Materials and Methods for details on inference using manufactured data). (**B** to **F**) Manufactured weekly influenza incidences (on a $\log_{10}$ scale). (**G** to **K**) Simulated weekly pneumococcal pneumonia incidences (on a $\log_{10}$ scale) using the MLE model and influenza cases as covariates. (**L** to **P**) Likelihood profiles of the susceptibility impact ϕ. The dashed red line is the actual value of interaction (ϕ = 85, MLE model), and the values of ϕ between the two dashed black lines are within 95% CI.

seasonal influenza peaks is typically below this level (Fig. 4A). Therefore, the examination of shorter data sets from time periods exhibiting little interannual influenza variability can fail to detect any meaningful interaction between influenza and pneumococcal pneumonia. Thus, the epidemiological signature of this strong but short-lived interaction appears modest, and its detectability in data relies on information provided by differential sizes of seasonal influenza outbreaks.

DISCUSSION

Many microbial pathogens associated with infectious diseases cocirculate in a population and can co-occur within individual hosts. Despite their ubiquity, detecting interactions between pathogens in a natural setting remains a challenge that general statistical approaches can fail to meaningfully identify (*7*, *34*, *35*). We have focused on two common and rela-

tively well-studied human pathogens: the influenza virus and the bacterium *S. pneumoniae*. Our research has used a framework for statistical inference using mechanistic models to characterize the interaction between two important infectious diseases with the aim of reconciling the contradictory conclusions of studies conducted at different scales. We have identified the nature of this interaction (enhanced susceptibility to pneumococcal pneumonia after recent infection with influenza), its magnitude, and time scale. In the process, we have unpacked the population-level implications of immune-mediated processes shown to occur at the level of the individual. This work highlights the potential power of using likelihood-based inferential approaches in conjunction with high-resolution data: In addition to providing results that have a mechanistic interpretation, these methods can often uncover underlying processes that are not necessarily visible to the naked eye.

In the absence of higher-resolution information, in particular age-stratified pneumococcal carriage (*36*, *37*) and serotype-specific incidence (*38*), our modeling choices have been pragmatic. The role of carriage in transmission and incidence of pneumococcal pneumonia is thought to be important (*36*, *37*), and we found similarly strong role of carriage-dependent transmission in our models (see section S-1.1 in the Supplementary Materials for discussion and estimates of carriage-dependent transmission). Furthermore, influenza has also been suggested to affect nasopharyngeal carriage of pneumococcal pneumonia (*39*). However, in the absence of carriage data and clear understanding of the casual link between carriage and transmission, we were unable to incorporate a dynamic and mechanistic description of carriage in this model and to explore possible effects of influenza on carriage. Our results may also have been affected by the use of hospitalization reports to infer and estimate interactions. Hospitalization data by definition represent infections at the severe end of the spectrum. Hence, the effect of influenza infection on the severity of subsequent pneumonia, as observed in animal experiments (*20*–*22*), may have been somewhat smaller in the data we examined.

Several of our findings are qualitatively consistent with outcomes in animal models. This body of experimental work has shown that, for instance, the influenza-pneumococcal interaction operates over a short window—5 to 7 days (*20*, *21*)—and that influenza can enhance susceptibility to pneumococcal infection (*23*, *24*). A number of candidate immunological mechanisms have been identified to explain the increased susceptibility (*9*, *21*). In animal models, increased susceptibility is quantified via the reduction in the pneumococcal infectious dose in subjects recently infected with influenza. The experimental observation that increased susceptibility translates into infectious doses that may be many orders of magnitude smaller (*20*) provides a mechanistic explanation for the MLE of our phenomenological parameter ϕ ~100.

Our work aims to bridge the understanding between pathogen interactions at two different scales, namely, at the scales of the host and the host population. Our approach here has been to infer interactions at the scale of the host from observations at the scale of the host population. For a relatively well-studied system, like the influenza-pneumococcal system, we argue that a framework that couples mechanistic models with statistical inference can achieve such a goal. In doing so, we also posit a possible mechanism by which potentially strong interactions between pathogens can be masked in nature.

MATERIALS AND METHODS

Data

Data sets I and II consisted of weekly hospitalization data from the state of Illinois, which we obtained from the State Inpatient Databases of the Healthcare Cost and Utilization Project (HCUP) (http://www.hcup-us.ahrq.gov/db/state/siddbdocumentation.jsp), maintained by the Agency for Healthcare Research and Quality (AHRQ), through an active collaboration between AHRQ and National Institutes of Health (NIH). This database contains all hospital discharge records from community hospitals in the state. HCUP databases bring together the data collection efforts of state data organizations, hospital associations, private data organizations, and the federal government to create a national information resource of patient-level health care data (*40*). Cases were identified by the presence of the relevant diagnostic codes listed anywhere in the patient's record, including pneumococcal pneumonia (International Classification of Diseases revision 9, code 481), influenza (487–488), or all-cause pneumonia, excluding influenza (480–486). Weekly time series were created for each disease outcome. Midyear population size estimates (fig. S1) for the state were obtained from the U.S. Census Bureau.

The weekly reports of influenza and pneumococcal pneumonia cases in data sets I and II span periods before and after the introduction of PCV, respectively. Data set I, as shown in Fig. 1A, spans from the middle of 1989 to the end of 1997, consisting of 442 weeks of data. Data set II, as shown in Fig. 1B, spans from the beginning of 2000 to the end of 2009, consisting of 520 weeks of data. Data are presented as incidences, based on the population of Illinois, which are shown in fig. S1.

Models

We present the complete model that was introduced in the Results section and was used for the inference of interaction. We proceed by first describing the deterministic skeleton of the model. Subsequently, we explain how seasonality and demography are incorporated, how the stochastic analog of the model is constructed, and finally, how the observation process is modeled.

Pneumococcal transmission and interaction with influenza

The equations below describe the deterministic skeleton of the pneumococcal transmission model and its interaction with influenza. The state variables are introduced in the Results section, and all the parameters including the MLE estimates are completely described in the Supplementary Materials (see table S2).

$$\frac{dS(t)}{dt} = \mu(N(t) - S(t)) - \lambda S_U(t) - \phi\lambda S_F(t) + \varepsilon R(t)$$
$$\frac{dI(t)}{dt} = \lambda(t) S_U(t) + \phi\lambda(t) S_F(t) - \gamma I(t) - \mu I(t)$$
$$\frac{dR(t)}{dt} = \gamma I(t) - \mu R(t) - \varepsilon R(t)$$
$$S_F(t) = \frac{F(t)}{\rho_F N(t)} S(t)$$
$$S_U(t) = S(t) - S_F(t) = S(t) - \frac{F(t)}{\rho_F N(t)} S(t)$$
$$\frac{dI_F(t)}{dt} = \phi\lambda(t) S_F(t) - \gamma I_F(t) - \mu I_F(t)$$
$$\lambda(t) = \beta(t)\left[\frac{I_U(t)}{N(t)} + \theta\frac{I_F(t)}{N(t)} + \omega\right]$$

Incorporation of seasonality and demography

The pneumococcal transmission is modeled to be seasonal. Seasonality is implemented using six cubic *b*-spline functions. We pay careful attention to estimating the shape of the seasonality accurately. This is reflected in the choice of flexible *b*-spline functions, with 6 basis.

Because we are fitting data at high resolution in time, it is important to estimate the shape of the seasonality function accurately. Within the pomp framework, this can be called by using periodic.bspline.basis and supplying time periods, degree, and the number of basis.

We also incorporate the population of Illinois, which is shown in fig. S1. The population data are treated as a covariate in these models, and the change in population is treated as excess birth that directly enters the susceptible compartment.

Stochastic analog

To model the presence of stochasticity, we translate the system of ordinary differential equations defined above into a stochastic process model. We do this by considering each flux between compartments to be a random process. In particular, we assume that, over a small time interval of duration Δt, the per capita rates are constant and that the fluxes out of each compartment are independent, multinomial random variables. Thus, for example, if we focus on the R compartment, there are two ways of exiting: loss of immunity and death. By assumption, the per capita probability of exit in the interval $(t, t + \Delta t)$ is constant and, letting $E_R(t)$ denote the number that actually exits R in this interval, we have $E_R \sim \text{Binomial}(R, 1 - \exp(-(\varepsilon + \mu)\,\Delta t))$. Among those that exit, the numbers of hosts respectively losing immunity and dying over this time interval are distributed as $\text{Multinomial}(R, \frac{\varepsilon}{\varepsilon+\mu}, \frac{\mu}{\varepsilon+\mu})$.

Finally, to model extrademographic stochasticity, we include a γ-distributed multiplicative white noise, $\mathrm{d}W/\mathrm{d}t$, in the transmission process (*30*, *41*). The standard deviation of this noise, β_{sd}, is also fit along with the parameters. The force of infection is given by the following equation:

$$\lambda(t) = \lambda(t)\left[\frac{I_U(t)}{N(t)} + \theta\frac{I_F(t)}{N(t)} + \omega\right]\frac{\mathrm{d}W}{\mathrm{d}t}$$

Measurement model

Pneumococcal pneumonia cases in all our data are reported at weekly interval. We model the observation process to match this frequency of data reporting. We define $H(t)$ to be the total number of new recoveries in week t, of which $H_F(t)$ are recoveries co-infected with influenza, and the remaining $H_U(t)$ are not. We assume that the weekly case reports, C_P, are normally distributed, that is,

$$C_P \sim N(\rho_p H, \sigma)$$

where ρ_p is the reporting ratio and σ is the standard deviation. We assume that the variance scales linearly with the mean, that is, $\sigma^2 = c^2\rho_p C_P$. The parameter related to the scaling of the standard deviation, c, is also fit along with other parameters.

To allow for differences in reporting in pneumococcal pneumonia because of the presence of influenza, we assume that the cases with influenza are ξ times more likely to be reported compared to those without influenza. This results in the following expansion of the above equation:

$$C_P \sim N(\rho_p(H_F + \xi H_U), \sigma)$$

Likelihood inference framework

For likelihood-based inference, we use the framework of partially observed Markov processes (*7*, *31*, *32*, *42*) that is implemented in a freely available software package pomp (*33*). This framework consists of the following four components:

(i) Data: These are weekly case reports of pneumococcal pneumonia between 1989 and 1997 for data set I and between 2000 and 2009 for data set II.

(ii) Covariates: We use weekly case reports of influenza matching the time period spanned by the data, and the population of Illinois as covariates.

(iii) The process model: The process model is proposed to describe the underlying epidemiological and demographic processes. This is described in the "Models" section of Materials and Methods.

(iv) The measurement model: The measurement model is proposed to describe the process by which the data are reported. This is described in the "Measurement model" section of Materials and Methods.

For a data set Y, consisting of observations of $y(t_j)$, $j = 1, \ldots, n$ at n points in time, we calculate the likelihood that a chosen parameter set θ explains the complete data (within the confines of the process and observation models). This likelihood function $L(\theta)$ is a product of conditional likelihoods, $L_{t_j}(\theta)$, calculated at each time t_j for all n data points in time. If $f(y|t,\theta)$ is the probability of observing the data $y(t)$ at time t, given parameters θ (measurement model), then the likelihood and log-likelihood functions are defined as follows:

$$\begin{aligned} L(\theta) &= f(y(t_1), y(t_2), \ldots, y(t_n)|\theta) \\ &= \prod_{j=1}^{n} f_\theta(y(t_j)|y(t_{j-1}), y(t_{j-2}), \ldots, y(t_1)) \\ &= \prod_{j=1}^{n} L_{t_j}(\theta) \\ \log L(\theta) &= \sum_{j=1}^{n} \log L_{t_j}(\theta) \end{aligned}$$

The Markov property of the model allows one to calculate the conditional likelihood $L_{t_j}(\theta)$ sequentially starting from $t_j = t_1$. For each t_j, the likelihood function is as follows:

$$\begin{aligned} L_{t_j}(\theta) &= f_\theta(y(t_j)|y(t_{1:j-1})) \\ &= f_\theta(y(t_j)|y(t_{j-1})) \\ &= \iint f_\theta(y(t_j)|x(t_j)) f_\theta(x(t_j)|x(t_{j-1})) f_\theta(x(t_{j-1})|y(t_{1:j-1}))\,\mathrm{d}x(t_{j-1}) \end{aligned}$$

Here, $x(t_j)$ represents the state of the complete system at time t_j. Consequently, $f_\theta(y(t_j)|x(t_j))$ is the measurement model, $f_\theta(x(t_j)|x(t_{j-1}))$ is the process model, and $f_\theta(x(t_{j-1})|y(t_{1:j-1}))$ is the filtering distribution. Furthermore, the calculation of the filtering distribution is simplified, identifying a recursive relation by applying Bayes' theorem.

$$\begin{aligned} f_\theta(x(t_{j-1})|y(t_{1:j-1})) &= \frac{f_\theta(y(t_{j-1})|x(t_{j-1})) f_\theta(x(t_{j-1})|y(t_{1:j-2}))}{\int f_\theta(y(t_{j-1})|x(t_{j-1})) f_\theta(x(t_{j-1})|t(t_{1:j-2}))\,\mathrm{d}x(t_{j-1})} \\ &= \frac{f_\theta(y(t_{j-1})|x(t_{j-1})) f_\theta(x(t_{j-1})|y(t_{1:j-2}))}{L_{t_{j-1}}(\theta)} \end{aligned}$$

The density functions $f_\theta(\cdot|\cdot)$ are calculated via sequential Monte Carlo particle filtering method (*42*, *43*).

The likelihood functions are optimized using mif algorithm, which is also implemented in pomp (*33*) package. For details pertaining to the methods and implementation of the algorithm, please refer to (*31*–*33*). The range of algorithm parameters used in the inference work is shown in table S1.

Influenza-attributable etiological fraction of pneumococcal pneumonia cases

Influenza-attributable etiological fraction of pneumococcal pneumonia cases in any time interval is taken to be the ratio of pneumococcal cases as a result of influenza to the total pneumococcal cases in the given time interval. Consider that $H(t)$ is the total number of new recoveries in week t, of which $H_F(t)$ are recoveries co-infected with influenza. With the normal reporting process, the reporting ratio ρ_P, and the standard deviation σ, the total reported cases are $C_P \sim N(\rho_P H_F, \sigma)$, and the total reported cases of pneumococcal infections with influenza are $C_P^F \sim N(\xi\rho_P H_F, \sigma)$. Recall, ξ is the hypothesized measure of severity impact. The influenza-attributable etiological fraction of pneumococcal pneumonia cases during week t, $E_F(t)$, is given by the following equation:

$$E_F(t) = \frac{C_P^F(t)}{C_P(t)}$$

For results presented in Fig. 3, we estimate C_P and C_P^F using separate MLE models for data sets I and II. Note that $\xi = 1$ in these MLEs. We use 1000 simulations of the MLE models to find the mean and the 95% CIs for these estimates.

Detectability experiments in manufactured data

To study the effect of variation in influenza on pneumococcal pneumonia incidence, and further on the ability to detect the enhancement effect, we manufacture several sets of influenza data, each taken to be weekly case reports of the same length (208 weeks, ~4 years). In 3 of 4 years, we set the influenza reports to the same level as seen in the 2000 to 2001 season in data set II. The remaining third season is varied between data sets. This is to reflect one central component of interannual variability in influenza, the height of the peak.

We then take the MLE model (corresponding to data set II, which predicts an 85-fold susceptibility enhancement) and generate simulated data sets of pneumococcal pneumonia cases for each of the influenza data sets. The population is taken to match the first 4 years in Illinois in data set II. Now, on the basis of pneumococcal pneumonia and influenza, we ask whether the same likelihood-based framework can detect susceptibility enhancement in each of the data sets. We attempt to infer ϕ, given that we have perfect knowledge of all of the other parameters. The likelihood profiles of ϕ from inference tests on five of such data sets are shown in Fig. 4.

SUPPLEMENTARY MATERIALS

www.sciencetranslationalmedicine.org/cgi/content/full/5/191/191ra84/DC1
Section S-1. Additional results.
Section S-2. A brief literature survey on influenza-pneumococcal interaction.
Section S-3. Sensitivity analyses.
Fig. S1. Population of Illinois.
Fig. S2. Likelihood profiles for carriage-related hazard and influenza reporting ratio.
Fig. S3. Simulations from the models fit to data set I.
Fig. S4. Simulations from the models fit to data set II.
Fig. S5. Comparisons between predictions and the data.
Fig. S6. Inference on the timing of the interaction.
Fig. S7. Schematic representation of the alternative model with vaccine.
Fig. S8. The inference for influenza-pneumococcal pneumonia interaction using the alternative vaccine model.
Fig. S9. Estimate of enhancement on various subsets of data set II.
Fig. S10. The effect of timing of influenza peaks on detectability.
Table S1. Parameters used in inference algorithm with their ranges.
Table S2. Model parameters and their estimated range for epidemiology of pneumococcal pneumonia.

REFERENCES AND NOTES

1. T. N. Petney, R. H. Andrews, Multiparasite communities in animals and humans: Frequency, structure and pathogenic significance. *Int. J. Parasitol.* **28**, 377–393 (1998).
2. P. Rohani, C. J. Green, N. B. Mantilla-Beniers, B. T. Grenfell, Ecological interference between fatal diseases. *Nature* **422**, 885–888 (2003).
3. J. Lello, B. Boag, A. Fenton, I. R. Stevenson, P. J. Hudson, Competition and mutualism among the gut helminths of a mammalian host. *Nature* **428**, 840–844 (2004).
4. R. Pullan, S. Brooker, The health impact of polyparasitism in humans: Are we under-estimating the burden of parasitic diseases? *Parasitology* **135**, 783–794 (2008).
5. E. C. Griffiths, A. B. Pedersen, A. Fenton, O. L. Petchey, The nature and consequences of coinfection in humans. *J. Infect.* **63**, 200–206 (2011).
6. S. Telfer, X. Lambin, R. Birtles, P. Beldomenico, S. Burthe, S. Paterson, M. Begon, Species interactions in a parasite community drive infection risk in a wildlife population. *Science* **330**, 243–246 (2010).
7. S. Shrestha, A. A. King, P. Rohani, Statistical inference for multi-pathogen systems. *PLoS Comput. Biol.* **7**, e1002135 (2011).
8. A. A. Bosch, G. Biesbroek, K. Trzcinski, E. A. M. Sanders, D. Bogaert, Viral and bacterial interactions in the upper respiratory tract. *PLoS Pathog.* **9**, e1003057 (2013).
9. J. A. McCullers, Insights into the interaction between influenza virus and pneumococcus. *Clin. Microbiol. Rev.* **19**, 571–582 (2006).
10. D. M. Morens, J. K. Taubenberger, A. S. Fauci, Predominant role of bacterial pneumonia as a cause of death in pandemic influenza: Implications for pandemic influenza preparedness. *J. Infect. Dis.* **198**, 962–970 (2008).
11. D. M. Weinberger, L. Simonsen, R. Jordan, C. Steiner, M. Miller, C. Viboud, Impact of the 2009 influenza pandemic on pneumococcal pneumonia hospitalizations in the United States. *J. Infect. Dis.* **205**, 458–465 (2012).
12. L. Simonsen, The global impact of influenza on morbidity and mortality. *Vaccine* **17** (Suppl. 1), S3–S10 (1999).
13. S. F. Dowell, C. G. Whitney, C. Wright, C. E. Rose Jr., A. Schuchat, Seasonal patterns of invasive pneumococcal disease. *Emerg. Infect. Dis.* **9**, 573–579 (2003).
14. N. D. Walter, T. H. Taylor Jr., S. F. Dowell, S. Mathis, M. R. Moore; Active Bacterial Core Surveillance System Team, Holiday spikes in pneumococcal disease among older adults. *N. Engl. J. Med.* **361**, 2584–2585 (2009).
15. C. G. Grijalva, J. P. Nuorti, P. G. Arbogast, S. W. Martin, K. M. Edwards, M. R. Griffin, Decline in pneumonia admissions after routine childhood immunisation with pneumococcal conjugate vaccine in the USA: A time-series analysis. *Lancet* **369**, 1179–1186 (2007).
16. D. B. Louria, H. L. Blumenfeld, J. T. Ellis, E. D. Kilbourne, D. E. Rogers, Studies on influenza in the pandemic of 1957-1958. II. Pulmonary complications of influenza. *J. Clin. Invest.* **38**, 213–265 (1959).
17. M. Lindsay Jr., E. Herrmann Jr., G. Morrow Jr., A. Brown Jr., Hong Kong influenza: Clinical, microbiologic, and pathologic features in 127 cases. *JAMA* **214**, 1825–1832 (1970).
18. A. L. Bisno, J. P. Griffin, K. A. Van Epps, H. B. Niell, M. W. Rytel, Pneumonia and Hong Kong influenza: A prospective study of the 1968-1969 epidemic. *Am. J. Med. Sci.* **261**, 251–263 (1971).
19. J. R. Gill, Z. M. Sheng, S. F. Ely, D. G. Guinee, M. B. Beasley, J. Suh, C. Deshpande, D. J. Mollura, D. M. Morens, M. Bray, W. D. Travis, J. K. Taubenberger, Pulmonary pathologic findings of fatal 2009 pandemic influenza A/H1N1 viral infections. *Arch. Pathol. Lab. Med.* **134**, 235–243 (2010).
20. J. A. McCullers, J. E. Rehg, Lethal synergism between influenza virus and *Streptococcus pneumoniae*: Characterization of a mouse model and the role of platelet-activating factor receptor. *J. Infect. Dis.* **186**, 341–350 (2002).
21. K. Sun, D. M. Metzger, Inhibition of pulmonary antibacterial defense by interferon-g during recovery from influenza infection. *Nat. Med.* **14**, 558–564 (2008).
22. I. Kukavica-Ibrulj, M. E. Hamelin, G. A. Prince, C. Gagnon, Y. Bergeron, M. G. Bergeron, G. Boivin, Infection with human metapneumovirus predisposes mice to severe pneumococcal pneumonia. *J. Virol.* **83**, 1341–1349 (2009).
23. J. A. McCullers, J. L. McAuley, S. Browall, A. R. Iverson, K. L. Boyd, B. H. Normark, Influenza enhances susceptibility to natural acquisition of and disease due to *Streptococcus pneumoniae* in ferrets. *J. Infect. Dis.* **202**, 1287–1295 (2010).
24. D. A. Diavatopoulos, K. R. Short, J. T. Price, J. J. Wilksch, L. E. Brown, D. E. Briles, R. A. Strugnell, O. L. Wijburg, Influenza A virus facilitates *Streptococcus pneumoniae* transmission and disease. *FASEB J.* **24**, 1789–1798 (2010).
25. N. D. Walter, T. H. Taylor, D. K. Shay, W. W. Thompson, L. Brammer, S. F. Dowell, M. R. Moore; Active Bacterial Core Surveillance Team, Influenza circulation and the burden of invasive pneumococcal pneumonia during a non-pandemic period in the United States. *Clin. Infect. Dis.* **50**, 175–183 (2010).

26. S. P. Kuster, A. R. Tuite, J. C. Kwong, A. McGeer; Toronto Invasive Bacterial Diseases Network Investigators, D. N. Fishman, Evaluation of coseasonality of influenza and invasive pneumococcal disease: Results from prospective surveillance. *PLoS Med.* **8**, e1001042 (2011).
27. A. Toschke, S. Arenz, R. von Kries, W. Puppe, J. Weigl, M. Höhle, U. Heininger, No temporal association between influenza outbreaks and invasive pneumococcal infections. *Arch. Dis. Child.* **93**, 218–220 (2008).
28. R. M. Anderson, R. M. May, *Infectious Diseases of Humans: Dynamics and Control* (Oxford Univ. Press, Oxford, 1991).
29. M. Keeling, P. Rohani, *Modelling Infectious Diseases* (Princeton University Press, Princeton, NJ, 2008).
30. C. Bretó, D. He, E. L. Ionides, A. A. King, Time series analysis via mechanistic models. *Ann. Appl. Stat.* **3**, 319–348 (2009).
31. E. L. Ionides, C. Bretó, A. A. King, Inference for nonlinear dynamical systems. *Proc. Natl. Acad. Sci. U.S.A.* **103**, 18438–18443 (2006).
32. A. A. King, E. L. Ionides, M. Pascual, M. J. Bouma, Inapparent infections and cholera dynamics. *Nature* **454**, 877–880 (2008).
33. A. A. King, E. L. Ionides, C. M. Breto, S. Ellner, B. Kendall, H. Wearing, M. J. Ferrari, M. Lavine, D. C. Reuman, pomp: Statistical inference for partially observed Markov processes (R package); http://pomp.r-forge.r-project.org.
34. C. Bottomley, V. Isham, M. G. Basáñez, Population biology of multispecies helminth infection: Interspecific interactions and parasite distribution. *Parasitology* **131**, 417–433 (2005).
35. A. Fenton, M. E. Viney, J. Lello, Detecting interspecific macroparasite interactions from ecological data: Patterns and process. *Ecol. Lett.* **13**, 606–615 (2010).
36. B. M. Gray, G. M. Converse III, H. C. Dillon Jr., Epidemiologic studies of *Streptococcus pneumoniae* in infants: Acquisition, carriage, and infection during the first 24 months of life. *J. Infect. Dis.* **142**, 923–933 (1980).
37. D. Bogaert, R. De Groot, P. W. Hermans, *Streptococcus pneumoniae* colonisation: The key to pneumococcal disease. *Lancet Infect. Dis.* **4**, 144–154 (2004).
38. D. M. Weinberger, Z. B. Harboe, E. A. Sanders, M. Ndiritu, K. P. Klugman, S. Rückinger, R. Dagan, R. Adegbola, F. Cutts, H. L. Johnson, K. L. O'Brien, J. A. Scott, M. Lipsitch, Association of serotype with risk of death due to pneumococcal pneumonia: A meta-analysis. *Clin. Infect. Dis.* **51**, 692–699 (2010).
39. S. Nakamura, K. M. Davis, J. N. Weiser, Synergistic stimulation of type I interferons during influenza virus coinfection promotes *Streptococcus pneumoniae* colonization in mice. *J. Clin. Invest.* **121**, 3657–3665 (2011).
40. HCUP SID Database Documentation, Healthcare Cost and Utilization Project (HCUP), Agency for Healthcare Research and Quality, Rockville, MD; http://www.hcup-us.ahrq.gov/db/state/siddbdocumentation.jsp.
41. D. He, E. L. Ionides, A. A. King, Plug-and-play inference for disease dynamics: Measles in large and small populations as a case study. *J. R. Soc. Interface* **7**, 271–283 (2010).
42. E. L. Ionides, C. Breto, A. A. King, *Modeling Disease Dynamics: Cholera as a Case Study* (Wiley, Hoboken, NJ, 2007), chap. 8, pp. 13–140.
43. M. S. Arulampalam, S. Maskell, N. Gordon, T. Clapp, A tutorial on particle filters for online nonlinear/non-Gaussian Bayesian tracking. *IEEE Trans. Signal Process.* **50**, 174–188 (2002).
44. D. M. Ferreira, K. C. Jambo, S. B. Gordon, Experimental human pneumococcal carriage models for vaccine research. *Trends Microbiol.* **19**, 464–470 (2011).
45. S. Cobey, M. Lipsitch, Niche and neutral effects of acquired immunity permit coexistence of pneumococcal serotypes. *Science* **335**, 1376–1380 (2012).
46. C. Reed, F. J. Angulo, D. L. Swerdlow, M. Lipsitch, M. I. Meltzer, D. Jernigan, L. Finelli, Estimates of the prevalence of pandemic (H1N1) 2009, United States, April–July 2009. *Emerg. Infect. Dis.* **15**, 2004–2007 (2009).
47. S. S. Shrestha, D. L. Swerdlow, R. H. Borse, V. S. Prabhu, L. Finelli, C. Y. Atkins, K. Owusu-Edusei, B. Bell, P. S. Mead, M. Biggerstaff, L. Brammer, H. Davidson, D. Jernigan, M. A. Jhung, L. A. Kamimoto, T. L. Merlin, M. Nowell, S. C. Redd, C. Reed, A. Schuchat, M. I. Meltzer, Estimating the burden of 2009 pandemic influenza a (H1N1) in the United States (April 2009–April 2010). *Clin. Infect. Dis.* **52** (Suppl. 1), S75–S82 (2011).
48. A. M. Presanis, D. De Angelis; New York City Swine Flu Investigation Team, A. Hagy, C. Reed, S. Riley, B. S. Cooper, L. Finelli, P. Biedrzycki, M. Lipsitch, The severity of pandemic H1N1 influenza in the United States, from April to July 2009: A Bayesian analysis. *PLoS Med.* **6**, e1000207 (2009).
49. J. F. Brundage, Interactions between influenza and bacterial respiratory pathogens: Implications for pandemic preparedness. *Lancet Infect. Dis.* **6**, 303–312 (2006).
50. G. A. Soper, The pandemic in the army camps. *JAMA* **71**, 1899–1909 (1918).
51. L. Robertson, J. P. Caley, J. Moore, Importance of Staphylococcus aureus in pneumonia in the 1957 epidemic of influenza A. *Lancet* **2**, 233–236 (1958).
52. R. Oseasohn, L. Adelson, M. Kaji, Clinicopathologic study of thirty-three fatal cases of Asian influenza. *N. Engl. J. Med.* **260**, 509–518 (1959).
53. S. W. Schwarzmann, J. L. Adler, R. J. Sullivan Jr., W. M. Marine, Bacterial pneumonia during the Hong Kong influenza epidemic of 1968-1969. *Arch. Intern. Med.* **127**, 1037–1041 (1971).
54. W. J. Shieh, D. M. Blau, A. M. Denison, M. Deleon-Carnes, P. Adem, J. Bhatnagar, J. Sumner, L. Liu, M. Patel, B. Batten, P. Greer, T. Jones, C. Smith, J. Bartlett, J. Montague, E. White, D. Rollin, R. Gao, C. Seales, H. Jost, M. Metcalfe, C. S. Goldsmith, C. Humphrey, A. Schmitz, C. Drew, C. Paddock, T. M. Uyeki, S. R. Zaki, 2009 pandemic influenza A (H1N1): Pathology and pathogenesis of 100 fatal cases in the United States. *Am. J. Pathol.* **177**, 166–175 (2010).
55. T. Mauad, L. A. Hajjar, G. D. Callegari, L. F. da Silva, D. Schout, F. R. Galas, V. A. Alves, D. M. Malheiros, J. O. Auler Jr., A. F. Ferreira, M. R. Borsato, S. M. Bezerra, P. S. Gutierrez, E. T. Caldini, C. A. Pasqualucci, M. Dolhnikoff, P. H. Saldiva, Lung pathology in fatal novel human influenza A (H1N1) infection. *Am. J. Respir. Crit. Care Med.* **181**, 72–79 (2010).
56. G. Palacios, M. Hornig, D. Cisterna, N. Savji, A. V. Bussetti, V. Kapoor, J. Hui, R. Tokarz, T. Briese, E. Baumeister, W. I. Lipkin, *Streptococcus pneumoniae* coinfection is correlated with the severity of H1N1 pandemic influenza. *PLoS One* **4**, e8540 (2009).
57. P. E. Kim, D. M. Musher, W. P. Glezen, M. C. Rodriguez-Barradas, W. K. Nahm, C. E. Wright, Association of invasive pneumococcal disease with season, atmospheric conditions, air pollution, and the isolation of respiratory viruses. *Clin. Infect. Dis.* **22**, 100–106 (1996).
58. K. Grabowska, L. Högberg, P. Penttinen, Å. Svensson, K. Ekdahl, Occurrence of invasive pneumococcal disease and number of excess cases due to influenza. *BMC Infect. Dis.* **6**, 58 (2006).
59. M. Watson, R. Gilmour, R. Menzies, M. Ferson, P. McIntyre; New South Wales Pneumococcal Network, The association of respiratory viruses, temperature, and other climatic parameters with the incidence of invasive pneumococcal disease in Sydney, Australia. *Clin. Infect. Dis.* **42**, 211–215 (2006).
60. D. R. Murdoch, L. C. Jennings, Association of respiratory virus activity and environmental factors with the incidence of invasive pneumococcal disease. *J. Infect.* **58**, 37–46 (2009).
61. A. G. Jansen, E. A. Sanders, A. M. van der Ende, A. W. van Loon, A. Hoes, E. Hak, Invasive pneumococcal and meningococcal disease: Association with influenza virus and respiratory syncytial virus activity? *Epidemiol. Infect.* **136**, 1448–1454 (2008).
62. D. J. Earn, P. Rohani, B. M. Bolker, B. T. Grenfell, A simple model for complex dynamical transitions in epidemics. *Science* **287**, 667–670 (2000).

Acknowledgments: We thank E. Ionides for input on the modeling work, M. Lipsitch for helpful suggestions, the Rohani and King laboratories for comments on the manuscript, and particularly A. A. King for several fruitful discussions over the course of this research. **Funding:** S.S. and P.R. were supported by the Vaccine Modeling Initiative of the Bill & Melinda Gates Foundation. P.R. also received support from the Research and Policy in Infectious Disease Dynamics program of the Science and Technology Directorate, Department of Homeland Security, the Fogarty International Center, NIH. **Author contributions:** Study conception: S.S., B.F., and P.R.; model development: S.S. and P.R.; model implementation: S.S.; data compilation: D.M.W., C.S., and C.V.; result analysis: S.S., B.F., D.M.W., C.V., and P.R.; writing: all authors. **Competing interests:** D.M.W. has received research support from Pfizer, the maker of the pneumococcal vaccine. The other authors declare that they have no competing interests.

Submitted 21 February 2013
Accepted 25 April 2013
Published 26 June 2013
10.1126/scitranslmed.3005982

Citation: S. Shrestha, B. Foxman, D. M. Weinberger, C. Steiner, C. Viboud, P. Rohani, Identifying the interaction between influenza and pneumococcal pneumonia using incidence data. *Sci. Transl. Med.* **5**, 191ra84 (2013).

Science Translational Medicine

Identifying the Interaction Between Influenza and Pneumococcal Pneumonia Using Incidence Data

Sourya Shrestha, Betsy Foxman, Daniel M. Weinberger, Claudia Steiner, Ccile Viboud, and Pejman Rohani

Sci. Transl. Med., **5** (191), .
DOI: 10.1126/scitranslmed.3005982

Tipping the Scales for Pathogen Interaction

As if it weren't bad enough to be infected by one pathogen, sometimes a primary infection can pave the way for a secondary infection as well. This has been thought to be the case with influenza virus and *Streptococcus pneumoniae*. Indeed, there are a lot of data in both humans and animal models that this does happen at the individual level. However, epidemiological studies measuring population-level effects do not reflect this observation. Now, Shrestha *et al.* use mathematical modeling of weekly incidence reports to reconcile these two seemingly disparate observations.

The authors constructed a mechanistic transmission model within a likelihood-based inference framework and characterized the timing, nature, and magnitude of the interaction between influenza virus and pneumococcal pneumonia. In individuals, they see that flu increases the susceptibility to subsequent pneumococcal pneumonia more than 100 times. However, at the population level, there is only a modest effect. These data suggest that influenza virus may contribute to pneumococcal pneumonia pathogenesis, but that these effects may be masked in the total population.

Science Translational Medicine (ISSN 1946-6242) is published by the American Association for the Advancement of Science. 1200 New York Avenue NW, Washington, DC 20005. The title *Science Translational Medicine* is a registered trademark of AAAS.